The physics of nanowire superconducting single-photon detectors

Renema, J.J.

Chapter 7

The Size of a Hotspot in Superconducting Single-Photon Detectors

We report on a preliminary set of data on a two-photon experiment to measure the size of an excitation area inside a superconducting nanowire single-photon detector. We find a size of the interaction area (i.e. 'hotspot size') of 22 ± 2 nm, which increases strongly at lower applied bias current. We find that this size is constant with photon energy. We find that in our tapered samples, detection events also occur up to approximately 70 nm away from the narrowest part of our wires.

7.1 Introduction

Superconducting single-photon detectors [1] are a crucial technology for a variety of applications [89]. One such application is multiphoton detection. In particular, superconducting bridges (called nanodetectors in this context) can be used for multiphoton subwavelength imaging [39], near-field multiphoton detection [118], and the measurement of ultrasensitive higher order autocorrelations [40], when biased with a critical current which is lower than the one used for single-photon detection. Simultaneous detection of up to six photons has been reported in the literature [40, 17].

The current model of photodetection in such detectors is as follows (see Chapters 1 and 4) [17, 28, 32, 72]: after the absorption of a photon, a cloud of quasiparticles is created. This cloud diffuses, spreading over some area of the wire. The redistribution of current towards the edges of the wire may cause a vortex to unbind from the edge of the wire, if the applied bias current

is sufficient. This causes a normal-state region to appear in the wire, which grows under the influence of Joule heating from the bias current, leading to a measureable voltage pulse and a detection event [9].

One of the earliest questions raised about the working mechanism of SSPDs was the size of the excitation made by the impinging photon, known as a hotspot. This question has particular relevance for multiphoton detection: if two photons are not absorbed sufficiently close to each other, no joint photodetection event will occur [44]. Therefore, the question of the hotspot size is crucial for interpreting multiphoton experiments, and for designing detectors that have optimal multiphoton detection properties.

In earlier work, attempts were made to determine the size of this hotspot by looking at the energy-current relation. Since the normal-core hotspot model (which was in use at the time) is essentially a geometric model, attempts were made to determine the size of the hotspot, by measuring the amount of current required to produce a detection event [66, 76, 119, 120]. This way of reasoning is in clear disagreement with the role of diffusion in the current models of the detection event, since the diffusion equation is linear in the initial excitation, i.e. one would expect the hotspot size to be independent of energy, whereas in the normal-core model this size increases as the square root of the energy. Moreover, the inferred size of the hotspot depends crucially on the assumed efficiency with which the energy of the initial photon is converted into quasiparticles.

In this chapter, we report preliminary work on determining the hotspot size[1] from a direct model-free measurement. Our strategy is to compare the efficiency of a detector in the one- and two photon regime. By comparing these efficiencies, we can find the distance which two photons have to be apart in order to produce a detection event. Reasoning classically, our technique relies on the fact that the first photon may be absorbed anywhere in the wire, whereas the second photon must be absorbed within some distance s_{hs} from the first. The hotspot size can therefore be extracted by comparing the efficiency in the one and two-photon regime.

We find a hotspot size which depends on the applied bias current. In the limit of high detection probability, we find that the size s_{hs} becomes constant at 22 ± 2 nm. We perform this experiment for four NbN detectors of 0, 100, 200 and 400 nm in length. At lower currents, this size increases, reaching a value of 200 nm for our two longest detectors. From this measurement we are able to infer which part of our wire is photodetecting. We find that the effective size of our detectors is 74 nm larger than their nominal size. We attribute this to photodetection events in the tapers of the

[1] We retain the terminology 'hotspot size' for consistency with previous work, even though this only has a meaning in the normal-state hotspot model, where the edges of the hotspot are sharply defined. We define the quantity which we are aiming to measure as the maximal distance with which two photons can be absorbed and still *jointly* (i.e. with a probability greater than they would have individually under the same circumstances) cause a detection event.

wire. This observation matches with previous results on the photodetecting area of zero-length bridges. We interpret these observations in terms of the diffusion-based vortex model. We discuss the implications of our results on the engineering of SSPDs as well as on their application as multiphoton detectors.

7.2 Experimental Setup

The detectors used in this experiment were patterned from a single film (5 nm NbN on GaAs) to ensure that the properties of the wires were as similar as possible. The film is deposited under an ambient temperature of 400 C, which was found to give the optimal critical current for NbN on GaAs. Under these conditions, the critical temperature of the film was 9.6 K, as opposed to 11 K for detectors grown at 440 C. The detectors were patterned using conventional e-beam lithography and reactive-ion etching in an SF_6 / Ar plasma. We fabricated detectors with lengths of 0, 100, 200 and 400 nm. For each length, we fabricated 16 nominally identical detectors, with a width of 150 nm.

In this experiment, we use a series of detectors which must differ only in the wire length. To find a group of similar detectors, we measured the critical current of these detectors in a probe station. One detector of each length was selected for further investigation for having similar critical current, between 27.4 and 27.9 μA. These detectors were located closely together on the sample, pointing to slowly varying properties within our film. After measurement of the critical current, we measured the quantum efficiency of these samples and found this to be of the order of 10^{-4}, which is the expected value taking into account the limited overlap between our illumination spot and the active area of the detector. Moreover, from the high and constant critical current, which is comparable to earlier samples[2] [39], and extensive inspection of detectors fabricated in the same process by SEM [121], we have minimized the possibility that these detectors are suffering from fabrication errors.

To characterize these detectors, we perform quantum detector tomography. We apply the usual technique of two crossed polarizers with a $\lambda/2$ wave plate in between to create variable attenuation of the incident light pulses with a dynamic range of more than 3 orders of magnitude. The axis of the second polarizer was set in such a way that the count rate on the devices was maximal, which corresponds to the TE polarization. This has the added advantage of producing the most uniform excitation probability density across the wire. We use a Coherent Vitesse laser ($\lambda = 800$ nm) to perform detector tomography. This laser is well suited for this experiment because it has a pulse duration of approximately 100 fs. Since the lifetime of an excitation in an SSPD is a few tens of ps [40], in this way we avoid

[2] See Chapters 2-4.

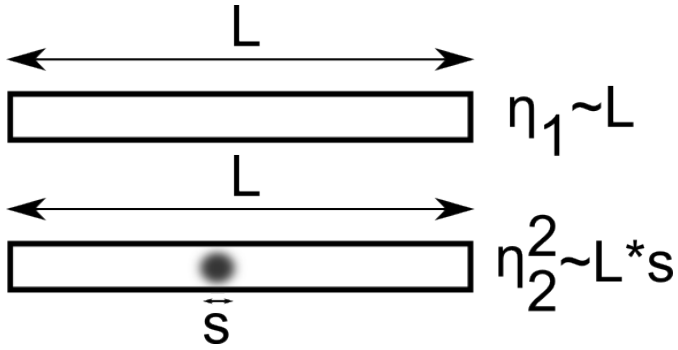

Figure 7.1: Relevant length scales in our experiment. The rectangle represents the detector, with an overall length L. The dot represents the quasiparticle excitation produced by the absorbed photon ('hotspot'), which has a length s.

introducing the temporal response of the device into the problem: our pulse duration is sufficiently short to act as a delta-like excitation compared to all relevant timescales.

7.3 Theory

In this section, we derive the expressions that we use to interpret our experimental data. For the two-photon efficiency, we compute the efficiency per photon, i.e. $\eta_{single} = \sqrt{\eta_{overall}}$, where $\eta_{overall}$ is the overall efficiency of the multiphoton process. The efficency per photon η_{single} is the quantity that is reported by our tomography protocol.

The geometry of our experiment and the length scales involved are shown in Figure 7.1. We show two cases: first, the absorption of a single photon, which can occur anywhere in the wire, and second, the absorption of two photons. We adopt a classical picure in which we may consider the photons as arriving sequentially. We need not consider photon bunching because the probability of two photons being absorbed by the same electron is minuscule, given that there are approximately 10^7 charge carriers in a 5 nm thick NbN film 200 by 150 nm in size [122]. For a one-photon event, the overall linear efficiency of the device is just proportional to the length of the device

$$\eta_1 \propto L. \tag{7.1}$$

For a two-photon event, the two photons must be absorbed within some distance s from each other, which represents the effective interaction distance between the photons which is the quantity of interest. The first photon can be absorbed anywhere in the wire, as in the single-photon case, but the

second photon effectively sees a smaller detector, of only length s. The overall efficiency for this process is therefore:

$$\eta_2^2 \propto Ls. \tag{7.2}$$

A comparison of the one and two-photon cases yields the hotspot size.

$$s = (\eta_2/\eta_1)^2 L, \tag{7.3}$$

which contains only measurable parameters on the right hand side of the equation.

This derivation containts two crucial assumptions: first, that the absorption probability across the detector is uniform. If this were not the case, we would have to consider each position individually. We satisfy this assumption by illuminating our detector with a light spot $w_{spot} \approx 0.2$ mm, which is much larger than the device itself, which has $L = 400$ nm and $w = 150$ nm for the largest device in this study.

The second assumption is that the influence of the hotspot extends across the width of the wire. In our model, two photons absorbed at the same position along the wire, but in different positions along the cross-section are counted as having $s_{hs} = 0$, i.e. we only count the distance along the wire. The motivation for this is that it is known that the influence of the hotspot in the form of redistributed current extends across the width of the wire. This justifies our assumption.

7.4 Results

Figure 7.2 shows the experimental results, for our 100 nm long sample. Quantum detector tomography enables us to separately determine both the absorption efficiency η and the internal detection probability for a given number of n photons p_n. This is done by using the count rate measurement at high intensity as a reference, assuming $p_n = 1$ for $n > n_{max}$, where n_{max} is some photon threshold, which can be determined via model selection. By performing quantum detector tomography (QDT), we find a regime where the detector primarily responds to single photons and a regime where the detector primarily responds to two-photon events. These regimes are demarcated by the high values of the detection probability p_1 and p_2, from I_b =20 - 24 μA and I_b =16 - 20 μA, respectively. We also find the efficiency in the one and two-photon regime. These results are consistent with results reported in Chapters 2-4.

We wish to compare linear efficiencies at currents at which the nonlinear internal detection probability of the wire is the same, using the nonlinear coeffcient as a measure of the location of the one- and two-photon regimes. We measure the distance between the one- and two-photon regime and observe that this value is independent of the chosen threshold criterion, i.e.

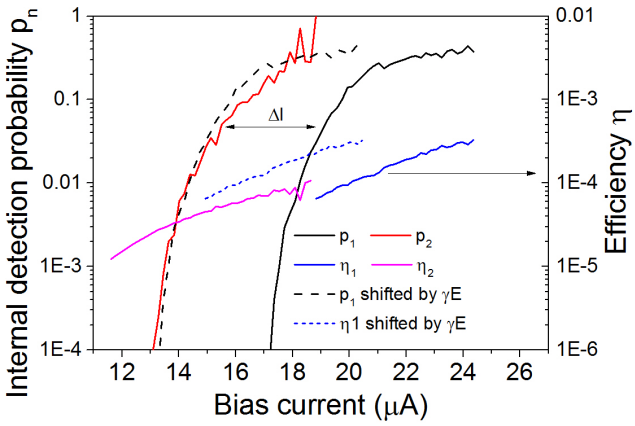

Figure 7.2: Experimental result of quantum tomography on a superconducting wire of 100 nm length. We find the efficiency as reported by our tomographic protocol in the one- and two-photon regime, as well as the coefficients p_1 and p_2 describing the internal nonlinear detection probabilities [67]. To compare the efficiency of the two photon regimes, we shift the efficiency curves by $\Delta I = \gamma E$ such that p_1 and p_2 overlap. This process is indicated by the arrow; the dotted lines show the shifted η and p_1.

that a simple shift in current serves to describe the difference between the one- and two-photon regime. This observation is consistent with the results presented in Chapter 2. We then apply this shift, such that the one- and two-photon regimes line up (dotted lines in Figure 7.2). Note the excellent agreement between p_2 and p_1 over more than three orders of magnitude.

Finally, to obtain the size of the hotspot, we divide the efficiency $\eta(I)$ by its shifted equivalent $\eta(I + \Delta I)$, obtaining the ratio η_2/η_1 of detection probabilities from equation 7.3. For each detector, we find that for detection probabilities in the range of $p_1 = 0.1 - 1$, the ratio is independent of the precise detection probability. We take this value as characteristic for that length of the detector. We then repeat this process for all four detectors.

Figure 7.3 shows the result of this procedure, for our four detectors of different lengths. We find qualitatively that the ratio η_2/η_1 decreases when increasing the length of the wire, as is expected from equation 7.3. We find, however, that the fit of equation 7.3 to our experimental data is poor: it overestimates the ratio η_2/η_1 for the 100 nm device. Moreover, it is completely unable to account for the finite value of η_2/η_1 for our zero-length detector. The observation that this detector has a finite probability for two-photon detection forces us to consider the tapers which lead to the device. These tapers are fabricated under a 45 degree angle and serve to lead the current into the active part of the wire without introducing too much current

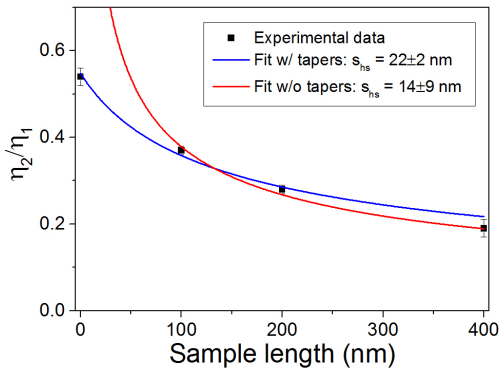

Figure 7.3: Result of the measurement of the hotspot size on a series of NbN detectors. The four data points are obtained by repeating the procedure outlined in Figure 7.2. The red line shows a fit of equation 7.3 to the experimental data, using the nominal length of the devices. The blue line shows a fit to the data taking into account an unknown extra length of the device, which represents the tapers leading to the narrow section of the bridge. For this fit, which has $\chi^2 = 3.6$, we find $s = 22 \pm 2$ nm and $l_{taper} = 74 \pm 12$ nm.

crowding.

To take into account the effect of the tapers, we replace the nominal value of L in equation 7.3 by $L + l_{taper}$, where l_{taper} is some characteristic length over which the leads of our system are also photodetecting, at the bias currents and detection probabilities which we are considering here. With this additional assumption, we are able to fit our data reasonably well ($\chi^2 = 3.6$). We find a value of $s_{hs} = 22 \pm 2$ nm, and a value of $l_{taper} = 74 \pm 12$ nm.

Figure 7.4 shows the dependence of the size of the hotspot on the overall detection probability. We find - suprisingly - that lower detection probabilities (i.e. lower currents) correspond to larger hotspots. Interestingly, we observe that the 0 nm brige deviates from the behaviour of the other devices at low detection probabilities. The 100 nm bridge follows the trend of the 200 nm and 400 nm bridge up until $s_{hs} \approx 75$ nm, and then deviates as well. We explain this result by pointing to the limited size of these devices; the 100 nm curve starts to deviate at the point where the size of a hotspot becomes comparable to the size of the detector. For the 200 and 400 nm bridges, we find values of s as large as 200 nm at $p_2 = 2 * 10^{-3}$, corresponding to $I_b = 13.5$ μA. Decreasing the current further, we arrive in the regime where three-photon detection events become dominant, and our analysis breaks down.

Figure 7.5 shows the dependence of the ratio η_2/η_1 on the wavelength of the incident photons, using a 100 nm long detector from a different film.

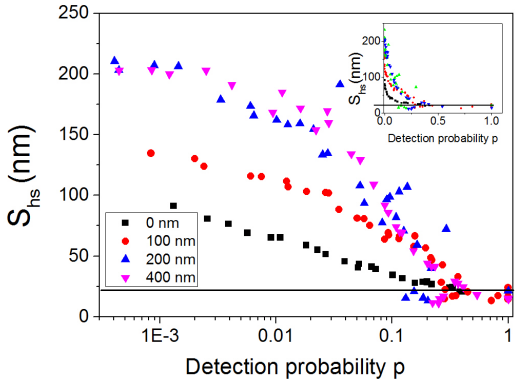

Figure 7.4: Dependence of hotspot size on detection probability. We plot the size of the hotspot as a function of the internal detection probability p_1. *Inset*: the same data as in the main figure, but plotted on a linear scale. In both the main figure and the inset, the black line indicates the hotspot size of $s_{hs} = 22$ nm, which is found in the limit of high detection probability.

For this experiment, we used a filtered Fianium supercontinuum laser, which has a specified pulse duration for its seed laser of 7 ps. We note that the observed value of η_2/η_1 is independent of photon energy. This is a strong indication of the role of diffusion in the detection process: since the diffusion equation is linear, this result can be interpreted in a very natural way in this context. In the normal-core model, in contrast, one would expect a $1/\sqrt{\lambda}$ dependence, which would mean almost a factor 2 difference over the wavelength range at which we performed experiments.

We note that the value of η_2/η_1 which is observed here is slightly higher than for the data reported on in Figures 7.1-7.4: if converted to a value for s using the same method, this would give a value of $s = 35$ nm. We note, however, that the laser used in this experiment has a temporal profile which is not well-suited to this experiment. In fact, it is expected that the pulse duration should depend on wavelength, increasing strongly with the difference $|\omega - \omega_{pump}|$, where ω is the frequency of the required light, and ω_{pump} is the pump frequency, to a value of several tens of ps[3] . We note that no evidence of this is visible in our measurements. Moreover, we note that the 100 nm detector used for this experiment was from a different film than the ones reported on above, which is known to give rise to larger fluctuations in properties than between detectors on the same film. We stress the preliminary character of these measurements.

Using the diffusion coefficient $D = 0.5$ cm^2/s, which is more or less constant for all SSPDs reported on in the literature, we may convert our

[3]This statement is based on private communication with Fianium Ltd.

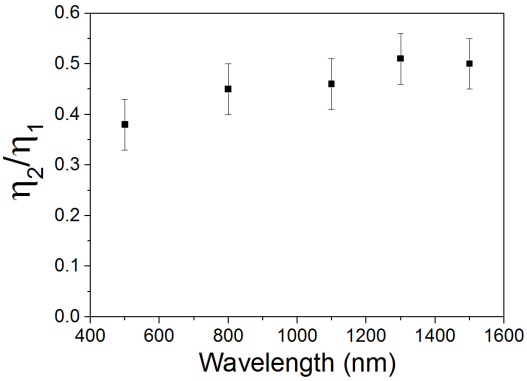

Figure 7.5: Values of η_2/η_1 for a 100 nm long device, measured with a filtered Fianium supercontinuum laser.

effective length to a time scale using the 2D-diffusion relation $s = \sqrt{Dt}$. For our high-detection probability value of $s = 22$ nm, we find $t_{hs} = 10 \pm 2$ ps. For the low-detection probability limit, we arrive at $t_{hs} = 800$ ps, which is comparable to the quasiparticle recombination time $t_r = 1000$ ps. We speculate that the recombination of quasiparticles could be the reason why the increase of the effective interaction distance saturates at 200 nm. More work at this point - especially on longer wires - is certainly necessary to obtain an answer to this question.

Next, we consider the observed detection probability dependence of s. By relying on the power-dependence of two-photon detection events, we postselect on those events where exactly two photons play a role. It is therefore natural to consider the quasiparticle density at a point inbetween the two photon absorption spots. Since diffusion occurs not only towards this point but in all directions, the quasiparticle density at the point where a detection event is supposed to occur will be lower for photons with high separation. If the required detection probability is lower, the absorption positions can therefore be further apart. This argument offers a qualitative explanation for the increase of s at lower detection probabilities, but a full theory would have to take into account the effect of the reduced bias current as well as all possible combinations of absorption positions.

Finally, we consider the measurement of the effective taper length $l_{taper} = 74 \pm 12$ nm. We consider three effects: the intrinsic spread in efficiency of the detector as a function of transverse position (which we considered in Chapter 5), the accuracy with which our constriction is defined, and the observed overall efficiency.

In Chapter 5, we demonstrated that the edges of the wire have a lower threshold current than the center part of the wire. This means that there

is a range of currents for which only the edges of the wire are efficiently photodetecting. This difference in threshold currents was calculated to be $\Delta I_{edge,center} = 0.14 I_c$, which is in reasonable agreement with the value of $\Delta I_{edge,center} \approx 0.2 I_c$ found experimentally. To make an order of magnitude estimate of the expected length over which the taper is still photodetecting, we adopt a zeroth-order approximation in which we consider the effect of the taper on the current density but not on any other photodetection properties of the wire. We find that the distance in the taper at which the edges of the wire are still photodetecting lies 30 nm away from the center of the constriction, pointing to a theoretical value of $l_{taper,th} = 60$ nm. Moreover, we must consider that at a given bias current, detection events in the taper will occur with lower probability, which we demonstrated results in a larger interaction length. We note, however, that this is a strong oversimplification as the photodetection will become less efficient because the wire is wider, which would lead to a lower estimate for l_{taper}.

Secondly, we must also consider the radius of curvature with which the central section of our zero-length bridge is defined, which is in the range of 5-10 nm. This would be added to any estimate of the photodetecting length. Thirdly, in Chapter 2, we measured a value of $\eta = 1.5 * 10^{-4}$ at high current for a detector nominally identical to this one. Taking the absorptance calculated in Chapter 5 and using the assumptions of uniform efficiency and illumination, we find $l_{taper} = 50$ nm. We therefore conclude that our measured value for the taper photodetection length is of the right order of magnitude.

7.5 Discussion

Multiphoton detectors suffer from overall low efficiency. Unfortunately, our results point to the fact that this efficiency cannot be strongly enhanced by increasing the length of the wire, at least for high detection probabilities. If the wire length is increased, the sample functions effectively as a series of independent nanodetectors one after each other, leading only to a linear enhancement in efficiency. A much better solution to enhance the multiphoton detection probability would be to introduce a thicker film for enhanced local absorption, or a cavity structure, since that enhances the absorption probability per photon, leading to quadratic instead of linear improvement in the two-photon regime.

The technological advantage of the low value of s_{hs} is that in any kind of spatially resolved two-photon imaging scheme, it is possible in principle to obtain far-subwavelength resolution using an appropriately current-biased nanodetector in two-photon mode. One could imagine, for example, running an asymmetric detector at such a current that only one edge is photodetecting. Then, one could sample the two-photon near field with a resolution of approximately 20 nm in one direction and some tens of nm in the other.

We demonstrated previously[4] that the detection probability depends strongly on the position along the cross-section of the wire where the photon is absorbed. This applies more strongly to multiphoton detection events. It is therefore clear that our measured length is an ensemble average of all possible pairs of absorption locations, weighted by the probability that those absorption locations produce a detection event. At very low detection probabilities, the overall detection probabilty is exponentially dominated by detection events at the edge of the wire. We therefore conclude that at low detection probability ($p \lesssim 0.05$) [35], we have measured the effective interaction length between photons which are absorbed at the edges of the wire.

We expect that the hotspot size which we have measured is a size along the length of the wire. The reason for this is as follows: since we must satisfy current continuity in the wire, an absorbed photon causes a disruption across the entire width of the wire. Apart from the corrections due to the inhomogeneity of the threshold current mentioned in the previous paragraph, we therefore expect that the interaction distance which we have measured is the component of the absorption distance along the length of the wire. Since the width of our wire is much smaller than the observed hotspot length, however, we can safely assume that hotspots are circular, assuming an isotropic diffusion constant. A full study of these problems would require a thorough sampling of all possible multiphoton absorption events, which could be done most efficiently through a Monte Carlo simulation. This is however beyond the scope of the present work.

We note that the position-dependent detection efficiency carries in it a length scale as well: from Figure 5.4, we observe that there is a plateau of low threshold currents at the edges of the curve, which is approximately 30 nm wide. Since the threshold current is reduced when the hotspot is in contact with the edge of the film, this provides another, more indirect measure of the hotspot size. This measurement is in reasonable agreement with the one presented here.

A experiment similar to ours was performed in WSi [123], where a constant, bias-current independent value of s_{hs} =100 nm was found. This result is supported by numerical simulations of quasiparticle multiplication and diffusion [32], which show that due to the lower density of states at the Fermi level and the lower gap, even a photon with a relatively small energy can make a significant part of the cross-section of the wire normal.

7.6 Conclusion

We have demonstrated a direct measurement of the hotspot size in a series of NbN superconducting single-photon detectors. We find a hotspot interaction size of 22 nm, which increases rapidly to a value of 200 nm when the detection

[4] See Chapter 5.

probability (or equivalently, the bias current) is decreased. We have shown that this length is independent of wavelength. We have interpreted this data in the context of the diffusion of quasiparticles. Our results show that far-subwavelength imaging with a suitably engineered SSPD is in principle possible.